Monte Carlo simulations of branched polymer surfaces without bending elasticity

Hiroshi Koibuchi,* Atsusi Nidaira, Takumi Morita, and Komei Suzuki
Department of Mechanical Engineering, Ibaraki College of Technology, Nakane 866 Hitachnaka, Ibaraki 312-8508, Japan
(Received 29 June 2002; revised manuscript received 24 March 2003; published 25 July 2003)

We study a model of elastic surfaces that was first constructed by Baillie *et al.* for an interpolation between the models of fluid and crystalline membranes. The Hamiltonian of the model is a linear combination of the Gaussian energy and a squared scalar curvature energy. These energy terms are discretized on dynamically triangulated surfaces that are allowed to self-intersect. We confirm that the model has not only crumpled phases but also a branched polymer phase, and find that the model undergoes a first-order phase transition between the branched polymer phase and one of the crumpled phases. We find also that the model undergoes a second- (or higher-) order phase transition between the branched polymer phase and another crumpled phase.

DOI: 10.1103/PhysRevE.68.011804 PACS number(s): 68.60.−p, 64.60.−i, 87.16.Dg

I. INTRODUCTION

Real membranes, such as bilayer lipid membranes, share common properties with phantom ones such as the Polyakov-Kleinert string [1,2]; both of them have surface tension and bending elasticity [3–6]. Hence, the real membranes [7–12] and the phantom ones [13–21] have been investigated numerically on triangulated surfaces by many groups with techniques similar to each other, although the real surfaces are self-avoiding, while the phantom surfaces are not. The phantom surface model has a crumpled phase at the bending rigidity $b\to 0$ and a smooth phase at $b\to\infty$. From the numerical studies done so far, it has been confirmed that there is a second-order phase transition of shape fluctuation between the smooth and the crumpled phases in the model of crystalline surfaces [7,8,13–15] where the bond connectivity is fixed and the lateral diffusion is absent. It was recently reported [21] that there is an expected second-order phase transition [22–25] also in the model of fluid surfaces where the vertices diffuse freely over the surface.

Baillie *et al.* [26–29] studied a fluid surface model for an interpolation between the models of the crystalline and the fluid surfaces. The Hamiltonian of the model contains an intrinsic scalar curvature term and the Polyakov-Kleinert (or Helfrich) energy terms. In the studies of Baillie *et al.*, it was found that the model has a branched polymer phase at intermediate values of interpolating parameter $\mu(\neq 0,\infty)$ when $b=0$. Thus, we recognize that when $b=0$ the model belongs to the crumpled phase at $\mu\to 0,\infty$, while it belongs to the branched polymer phase at intermediate values of μ. However, phase transitions between these phases remained to be studied.

In this paper, we study by Monte Carlo (MC) the phase transitions of the model first constructed by Baillie *et al.* for an interpolation of the crystalline and the fluid surfaces both of which can be viewed as discrete models of the Polyakov-Kleinert string.

We will find that there is a first-order phase transition of shape transformation between the branched polymer phase and one of the crumpled phases. Moreover, we find that the model undergoes a second- (or higher-) order phase transition characterized by the divergence of the specific heat for the intrinsic scalar curvature at $N\to\infty$. We expect that the model of Baillie *et al.* can be applied to studies on models of shape transformations of real membranes.

II. THE MODEL

A. Statistical mechanical model

A sphere in $\mathbf{R}^3$ is discretized with piecewise linear triangles. The spherical topology is assumed for neglecting the boundary of surfaces. We are not aimed at constructing a model of micellar aggregates of spherical topology in aqueous solutions. Each vertex has the three dimensional degrees of freedom represented by $X_i(\in\mathbf{R}^3)$. Every vertex is connected to its neighboring vertices by bonds, which are the edges of triangles.

The Gaussian energy S_1 and the scalar curvature energy S_3 are defined by

$$S_1=\sum_{(ij)}(X_i-X_j)^2,\quad S_3=\sum_i(6-\sigma_i)^2, \tag{1}$$

where $\Sigma_{(ij)}$ is the sum over all bonds (ij), and σ_i in S_3 is the total number of bonds emanating from the vertex i and is called the coordination number.

The partition function is defined by

$$Z=\sum_{\mathcal{T}}\int\prod_{i=1}^{N-1}dX_i\exp[-S(X,\mathcal{T})], \tag{2}$$

$$S(X,\mathcal{T})=aS_1+\mu S_3,\quad a=1,$$

where $\Sigma_{\mathcal{T}}$ denotes the sum over all possible triangulations $\mathcal{T}$. The Nth vertex is fixed to remove the translational zero mode of the surface; alternatively, the center of the surface can be fixed. The $S(X,\mathcal{T})$ shows that the Hamiltonian S explicitly depends on the variables X and $\mathcal{T}$. The coefficient a is called the surface tension, and it is assumed to be $a=1$. The symbol μ is the interpolating parameter. The partition function depends on μ: $Z=Z(\mu)$. The surfaces are allowed to self-intersect.

*Electronic address: koibuchi@mech.ibaraki-ct.ac.jp

It should be noted that our choice $a=1$ represents not only a redefinition of μ as μ/a but also a choice of the unit of length as $\sqrt{kT/a}=1$. Hence, the unit of μ becomes kT/a. We can choose the unit of length as $\sqrt{kT/a}=1$, because the partition function of Eq. (2) is scale invariant. The units will be explicitly mentioned if necessary.

The specific heat is defined by

$$C_{S_3}=(\mu^2/N)\partial^2 \log Z/\partial\mu^2,$$

and is practically calculated by using

$$C_{S_3}=\frac{\mu^2}{N}\langle (S_3-\langle S_3\rangle)^2\rangle, \tag{3}$$

hence it corresponds to the fluctuation of S_3.

A phase transition is called the nth order if the derivatives below the $(n-1)$th order of the free energy $F=-\log Z(\mu)$ are continuous and a derivative of the nth order is discontinuous. It should also be noted that a singular function, which is a function divergent somewhere in the parameter space, is a discontinuous function.

B. Squared scalar curvature S_3

Here we comment on S_3 in Eq. (1). If the Gaussian curvature K is integrated over a compact surface, the integration of K becomes a constant that depends only on the genus of the surface. For this reason, K is independent of the shape of membranes.

However, the integration of K^2 can play a nontrivial role in the shape transformation of membranes. In fact, the integration of K^2 has different values on surfaces, which are different in shape, even though the surfaces have the same genus.

It should be noted that S_3 in Eq. (1) is considered as a discretization of K^2. To see this, let us define the deficit angle δ_i by

$$\delta_i=2\pi-\sum_j \phi_j \tag{4}$$

at the vertex i, where ϕ_j denote the vertex angles of the triangles connected to the vertex i. This δ_i is considered as a discretization of the Gaussian curvature K (or the scalar curvature R). In fact, it is well known that the relation $\Sigma_i\delta_i=2\pi(2-\tau)$ is obtained by summing δ_i over a surface of genus τ. This is considered as a discrete version of the Gauss-Bonnet theorem $\int d^2x\sqrt{g}K=2\pi(2-\tau)$ for the compact surfaces of genus τ.

By proceeding this discretization further, we can also rewrite the right-hand side of Eq. (4) as $\Delta_i=6-\sigma_i$. This Δ_i can be interpreted as a discretization of K upto a multiplicative constant because of the relation $\Sigma_i\delta_i=2\pi\Sigma_i\Delta_i$. Thus, we obtain S_3 in Eq. (1) from $\int d^2x\sqrt{g}K^2$.

C. Monte Carlo technique

Spherical surfaces in $\mathbf{R}^3$ are discretized with the Voronoi triangulation [30], and they are used as the starting configurations of MC. The radii of the initial spheres are fixed so that the sum of the resulting squared length of bonds per vertex, i.e., the Gaussian energy per vertex $\Sigma_i l_i^2/N$ becomes almost equal to the expected value $\frac{3}{2}$. This value is obtained by the scale invariance of the partition function Z of Eq. (2). In fact, by letting $Z(\alpha):=\Sigma_{\mathcal{T}}\int\Pi_{i=1}^{N-1}dX_i\exp[-(\alpha S_1+\mu S_3)]$, we have $\langle S_1\rangle=-\partial(\log Z)/\partial\alpha(\alpha=1)$. Since $Z(\alpha)$ is scale invariant, replacing X by $\alpha^{-1}X$ in $Z(\alpha)$ we obtain $Z(\alpha)=\alpha^{-3(N-1)}\Sigma_{\mathcal{T}}\int\Pi_{i=1}^{N-1}dX_i\exp[-(\alpha S_1+\mu S_3)]$, and therefore we obtain $\langle S_1\rangle=3(N-1)/2$. Thus, we have $\langle S_1\rangle/N=3(N-1)/2N\simeq\frac{3}{2}$.

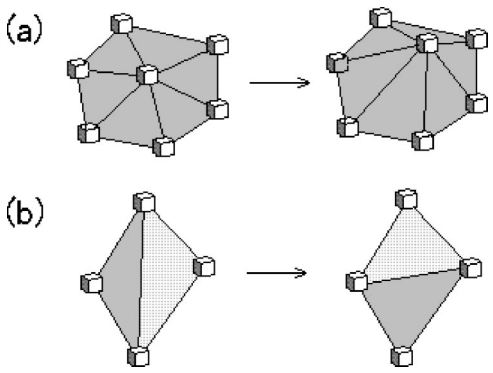

FIG. 1. Basic MC processes for (a) update of X, a small change of the position of a vertex, and (b) update of $\mathcal{T}$, a flip of a bond. Cubes represent vertices.

The basic MC processes are shown in Fig. 1. The positions X of the vertices and the triangulation $\mathcal{T}$ are updated using the canonical MC technique. Each position and network link is updated sequentially, with the change in connectivity following the fluid membrane algorithm developed by Baumgartner and Ho [9,10] and at the same time by Catterall [19]. X is updated so that $X'=X+\delta X$, where the small change δX is made at random in a small sphere centered at X. The radius δr of the small sphere is chosen to maintain the rate of acceptance r_X for X update to be $0.5\leqslant r_X\leqslant 0.55$. The δr is defined by using a constant number ϵ adjusted by hand as an input parameter so that $\delta r=\epsilon\langle l\rangle$, where $\langle l\rangle$ is the mean value of bond length computed at every 250 sweeps. It should be noted that δr becomes almost fixed because $\langle l\rangle$ is almost constant in the equilibrium configurations. Contrastingly, the rate of acceptance $r_{\mathcal{T}}$ for the flip of bonds is uncontrollable. The value of $r_{\mathcal{T}}$ is fixed automatically depending on the interpolating parameter μ in Eq. (2); it varies with the value of S_3 and will be discussed in the following section.

One MC sweep consists of N trials for X update and N trials for $\mathcal{T}$ update. Two consecutive N trials for X update and $\mathcal{T}$ update make one MC sweep.

No restrictions are imposed on the trial updates, except the minimum length of bonds, which corresponds to a hard core between the vertices at two ends of the bonds; whereas all the vertices that have no common bond are able to occupy even an identical position. Practically, the trial updates for X and $\mathcal{T}$ in Fig. 1 are made so that the resulting lengths of bonds should not be smaller than $10^{-6}\langle l\rangle$, where $\langle l\rangle$ is the mean value of bond length. The maximum number is not

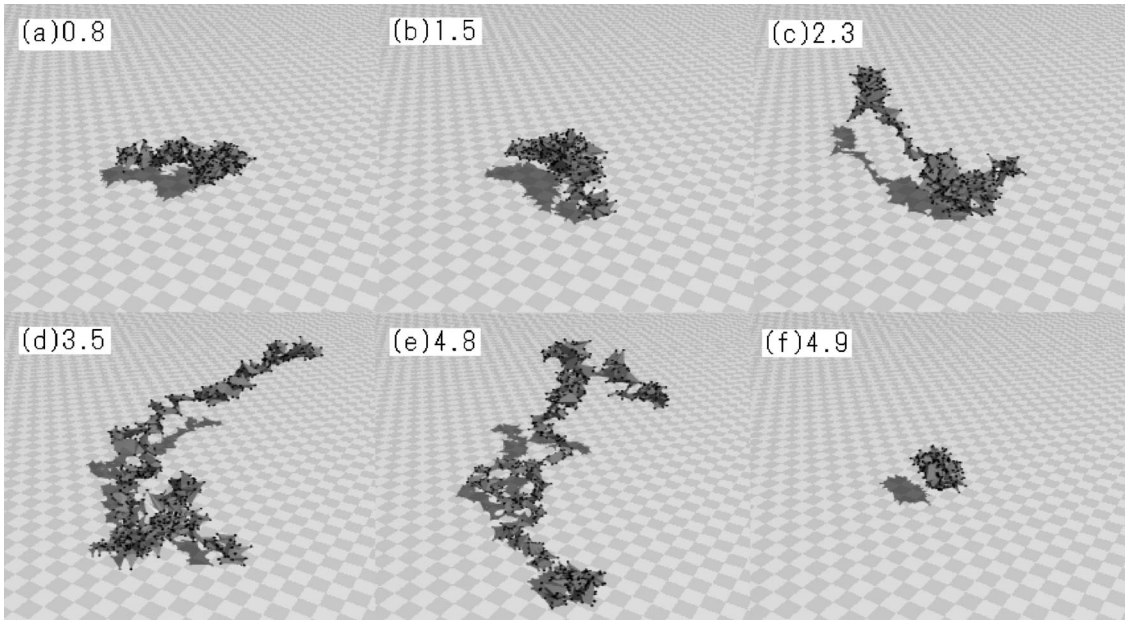

FIG. 2. Snapshots of surfaces of $N=1000$ in the equilibrium configurations at (a) $\mu=0.8$, (b) $\mu=1.5$, (c) $\mu=2.3$, (d) $\mu=3.5$, (e) $\mu=4.8$, and (f) $\mu=4.9$. Small spheres on the surfaces are the vertices.

imposed on the coordination number, while the minimum coordination number should be obviously 3.

It should be noted that the mean value of bond length in the equilibrium configurations is a constant in the unit of a/kT, which is assumed to be $a/kT=1$, as mentioned in Sec. II A. Thus, the minimum bond length that is the radius of the hard core becomes a constant. According to our experiences, the results of MC calculations are independent of a minimum bond length if it is small enough.

III. RESULTS

A. Snapshots of $N=1000$ surfaces

Figures 2(a)–2(f) are the snapshots of surfaces obtained at $\mu=0.8\sim4.9$, where $N=1000$. They were obtained after enough MC sweeps for the equilibrations started from a sphere as the starting configuration. These figures suggest that the membrane belongs to the branched polymer phase at $2.3\leqslant\mu\leqslant4.8$ and belongs to the crumpled phase both at $\mu<2.3$ and at $\mu>4.9$ when $N=1000$.

B. Results of $N=340$ surfaces

Figures 3(a) and 3(b) show the rate of acceptance $r_{\mathcal{T}}$ for the bond flip and the energy S_3 per vertex, respectively. $r_{\mathcal{T}}$ is uncontrollable in MC if S_3 is not contained in the Hamiltonian. However, if the Hamiltonian contains S_3 one can control $r_{\mathcal{T}}$ in MC, as shown in Fig. 3(a). The data denoted by the open (solid) circles are obtained by increasing (decreasing) the value of μ in MC started at $\mu=0.3$ ($\mu=6.7$). The starting configuration at every μ is the final one obtained at the previous μ. 2×10^6 sweeps are discarded for the thermalization at every μ, and S_3 is sampled at every 500 sweeps in the following 1.8×10^7 sweeps. We can see a kind of hysteresis at $\mu\simeq4$ in Figs. 3(a) and 3(b).

Figure 4(a) shows the specific heat C_{S_3}. We find that there are not only two peaks at $\mu\simeq0.4$ and at $\mu\simeq2.3$ but also a gap at $\mu\simeq4$ in C_{S_3}. Since the peak at $\mu\simeq0.4$ is very small, we will concentrate only on the peak at $\mu\simeq2.3$ and the gap at $\mu\simeq4$.

Figure 4(b) shows the mean square size X^2 defined by

$$X^2=\frac{1}{N}\sum_i (X_i-\overline{X})^2, \quad \overline{X}=\frac{1}{N}\sum_i X_i. \tag{5}$$

We find from Fig. 4(b) that X^2 significantly depends on μ and abruptly changes at $\mu\simeq4$, where C_{S_3} has the gap, as shown in Fig. 4(a). This suggests that there is a strong

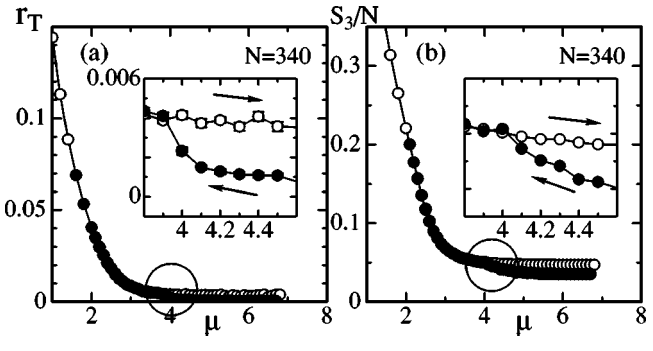

FIG. 3. (a) The rate of acceptance $r_{\mathcal{T}}$ for bond flips and (b) the squared scalar curvature per vertex S_3/N. The open circles (○) denote the data obtained by increasing the value of μ in MC started at $\mu=0.3$, while the solid circles (●) denote the data obtained by decreasing the value of μ in MC started at $\mu=6.7$. The starting configuration at each μ was the final one obtained at the previous μ. The unit of μ is kT/a.

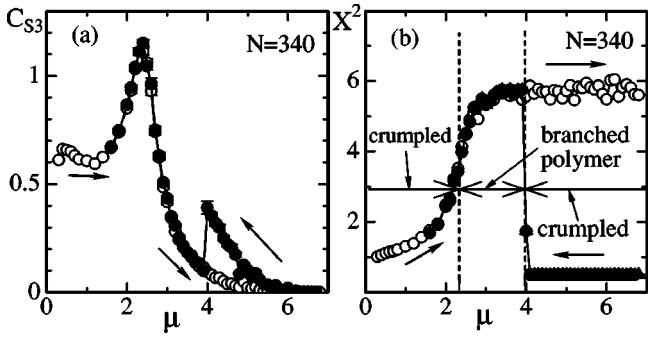

FIG. 4. (a) The specific heat C_{S_3} and (b) the mean square size X^2. The number of vertices is $N=340$. The units of C_{S_3}, X^2, and μ are $(kT/a)^2$, kT/a, and kT/a, respectively.

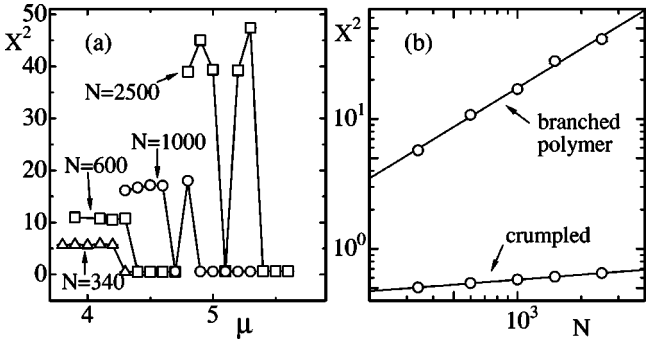

FIG. 5. (a) X^2 vs μ at the vicinity of critical points $\mu_c(N)$ of the first-order phase transition. (b) Log-log plots of mean values of X^2 vs N at $\mu<\mu_c(N)$ (branched polymer) and at $\mu>\mu_c(N)$ (crumpled). The unit of X^2 is kT/a, which is identical with that of μ.

(maybe the first order) phase transition between the branched polymer phase and the crumpled phase emerged at $\mu\geqslant 4$ for $N=340$.

We easily find from Fig. 4(b) that the crumpled phase emerges both at $\mu\to 0$ and at $\mu\to\infty$. Hence, the model contains two phase boundaries; one of which separates the branched polymer phase and the crumpled phase at $\mu\to\infty$, and the other separates the branched polymer phase and the crumpled phase at $\mu\to 0$. The dashed lines drawn vertically in Fig. 4(b) denotes these phase boundaries. We can see the peak of C_{S_3} and the gap of it just at these two phase boundaries, respectively, in Fig. 4(a).

Additional 6×10^8 MC sweeps were done at $\mu=7$ by starting with the final configuration corresponding to the symbol (○) at $\mu=7$ plotted in both Figs. 3 and 4. However, the obtained value of X^2 remains unchanged. In the same way, 6×10^8 sweeps were done at $\mu=6.7$ by starting with the sphere of radius R_0 chosen, so that $S_1\simeq\frac{3}{2}N$. We find in this case that the obtained surface remains crumpled, and that the value of X^2 remains a constant value, which is identical with that (●) at $\mu=6.7$ in Fig. 4(b). These indicate that the surface can hardly shrink even in the crumpled phase if it is once stretched, and also that the surface remains crumpled in the crumpled phase if it is once crumpled.

C. First-order phase transition

It was suggested in Figs. 3 and 4 that the phase transition between the branched polymer and one of the crumpled phases is of the first order. In this subsection, we will show more clearly and confirm this.

Figure 5(a) shows that X^2 discontinuously reduces to $X^2\simeq 0.5$ at $\mu=\mu_c(N)$ when μ increases. X^2 at $\mu<\mu_c(N)$ depends on N, and becomes larger and larger when N increases. While at $\mu>\mu_c(N)$, X^2 seems independent of N and becomes constant value: $X^2\simeq 0.5$. This suggests that the value of Hausdorff dimension H defined by

$$X^2\sim N^{2/H} \tag{6}$$

becomes very large at $\mu>\mu_c(N)$, while it remains small at $\mu<\mu_c(N)$. The critical points $\mu_c(N)$ of the phase transition are $\mu_c(340)\simeq 4.3$, $\mu_c(600)\simeq 4.4$, $\mu_c(1000\leqslant N\leqslant 1500)=4.8\sim 5$, and $\mu_c(N=2500)\simeq 5.5$, some of which can be viewed in Fig. 5(a).

Figure 5(b) shows X^2 just above and below $\mu_c(N)$ vs N in log-log scale. These X^2 are mean values obtained from the data points obtained at the vicinity of $\mu_c(N)$ for $N=340, 600, 1000, 1500, 2500$. The values of X^2 obtained just below $\mu_c(N)$ is denoted by *branched polymer* in the figure, while those just above $\mu_c(N)$ by *crumpled*.

Both of the straight lines in Fig. 5(b) are obtained by fitting the data to Eq. (6). Thus, we have

$$H_{\text{b.p.}}=1.93\pm 0.06,\quad H_{\text{cru}}=15.43\pm 0.28, \tag{7}$$

where $H_{\text{b.p.}}$ and H_{cru} correspond to H at the branched polymer phase and H at the crumpled phase, respectively, at the vicinity of the critical point.

The number of MC sweeps done at the vicinity of the critical points are 6×10^8 for $N=340, 600$, and $0.5\times 10^9\sim 1\times 10^9$ for $N=1000, 1500, 2500$. The number of thermalization sweeps done in the branched polymer phase is 1×10^7 for all values of N, while it is quite large (5×10^8, for example) at close vicinity of the critical points. After the thermalization, time series $\{S_3\}$ are sampled at every 500 sweeps, i.e., the number of sampling sweeps is 500. The starting configuration of MC at each μ is the sphere of radius $R(N)$ chosen so that $S_1/N\simeq 3/2$.

It should be noted that the results are almost independent of the sampling sweeps. The sampling sweeps of 500 is very smaller than a correlation time, which can be estimated as the minimum number of sweeps so that the autocorrelation coefficient

$$A(X^2)=\frac{\sum_i X^2(\tau_{i+1})X^2(\tau_i)}{\sum_i [X^2(\tau_i)]^2}$$

$$(\tau_{i+1}=\tau_i+n\times 500,\ n=1,2,\ldots)$$

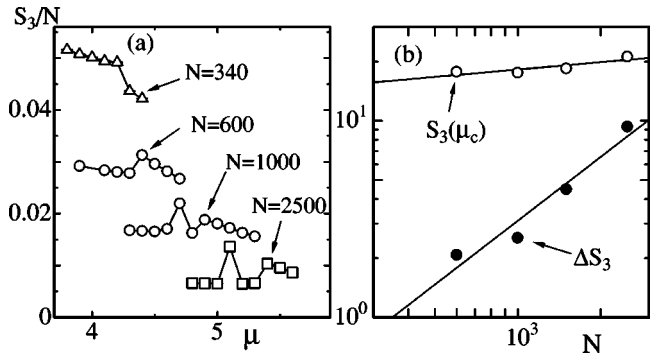

FIG. 6. (a) S_3/N vs μ at the vicinity of the first-order phase transition and (b) $S_3(\mu_c)$ (○) and the gap ΔS_3 (●) vs N in log-log scale, where $S_3(\mu_c)$ and ΔS_3 are defined by $S_3(\mu_c)=\frac{1}{2}[S_3(\mu>\mu_c)+S_3(\mu<\mu_c)]$ and $\Delta S_3=S_3(\mu>\mu_c)-S_3(\mu<\mu_c)$, respectively. The unit of μ is kT/a.

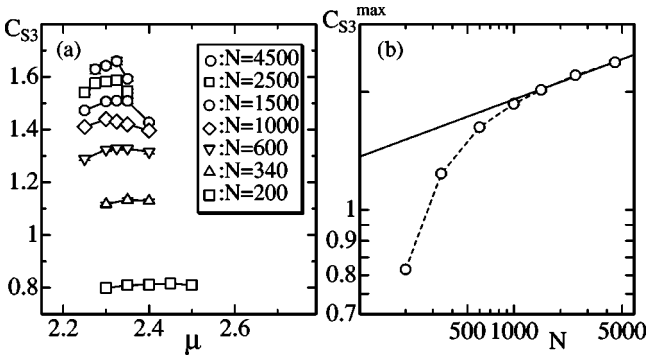

FIG. 7. (a) C_{S_3} vs μ and (b) the peaks $C_{S_3}^{\max}(N)$ vs N in log-log scale. The units of C_{S_3} and μ are $(kT/a)^2$ and kT/a, respectively.

becomes $A(X^2)\leqslant 0.1$. Nevertheless, we can see that the MC results are almost independent of the sampling sweeps [15,20,21].

The X^2 plotted in Fig. 5(a), which were obtained from the surfaces of $N=1000$, 2500, are fluctuated at close vicinity of the critical points. It appears that the X^2 is not well defined there. This ill definedness will be seen also in S_3 and in the specific heat C_{S_3}.

This ill definedness of X^2 seems due to the noncompact nature of the phase space $\mathbf{R}^3$ for the dynamical variable X. If the variables X are localized once at a stretched one-dimensional region in $\mathbf{R}^3$ to form a branched polymer surface, the surface can hardly shrink to a crumpled one, because all the variables X located at the stretched one-dimensional region cannot simultaneously move to a small region in $\mathbf{R}^3$ within finite MC sweeps. On the contrary, almost all the surfaces in the branched polymer phase can eventually stretch out and change into branched polymer surfaces after many thermalization sweeps, even when the surfaces are crumpled at the beginning.

Figure 6(a) shows that S_3/N, which is the internal energy per one vertex, has a gap at the critical points $\mu_c(N)$ when $N\geqslant 600$. This also suggests that the branched polymer phase and the crumpled phase are separated by a first-order phase transition. The continuous behavior seen in S_3 of $N=340$ seems due to the size effect, that is, the size of the surface is too small for low-frequency modes (or excitations) in the fluctuations of S_3. It also appears that the S_3 is not well defined at the critical points, as X^2 is not, when $N\geqslant 1000$.

A scaling property of the gap of S_3 at $N\to\infty$ is unclear in Fig. 6(a), because S_3 are divided by N in Fig. 6(a). Hence, we show $S_3(\mu_c)$ (○) and ΔS_3 (●) vs N in Fig. 6(b) in log-log scale, where $S_3(\mu_c)$ is defined by using S_3 just below and above $\mu_c(N)$, so that $S_3(\mu_c)=\frac{1}{2}[S_3(\mu>\mu_c)+S_3(\mu<\mu_c)]$, and ΔS_3 is the gap of S_3 at $\mu_c(N)$ defined by $\Delta S_3=S_3(\mu>\mu_c)-S_3(\mu<\mu_c)$.

We consider that the phase transition is characterized also by a discontinuity of S_3, because we can expect that $\Delta S_3\neq 0$ at $N\to\infty$ from Fig. 6(b). It should be noted that it is very hard to obtain S_3 precisely near the critical point because S_3 is not well defined at the critical point. This is the reason why the obtained data ΔS_3 considerably fluctuate in Fig. 6(b).

D. Continuous phase transition

It was suggested in Fig. 4(a) that the model undergoes a second-order phase transition at $\mu\simeq 2.3$. Hence, we will study this phase transition further using surfaces of larger N than $N=340$.

Figure 7(a) shows the specific heats C_{S_3} vs μ. The peak values $C_{S_3}^{\max}(N)$ of the specific heat against N are plotted in Fig. 7(b) in log-log scale to see whether $C_{S_3}^{\max}(N)$ is divergent or not, where $200\leqslant N\leqslant 4500$.

The number of MC sweeps done at the vicinity of the peaks of C_{S_3} are 3×10^8 for $N=600$, 1000, 1500, and 9×10^8 for $N=2500$, 4500. The thermalization sweeps done at every μ are 1×10^7 for $N=600$, 1000, 1500 and 4×10^7 for $N=2500$, 4500. The sampling sweeps and the starting configurations of MC are the same as those in the MC for the first-order phase transition presented in Sec. III C.

If we consider that $C_{S_3}^{\max}(N)$ scales according to

$$C_{S_3}^{\max}\sim N^{\sigma}, \tag{8}$$

when $N\geqslant 1500$, we find that the fluctuation of S_3 is divergent at $N\to\infty$, where σ is a critical exponent of the phase transition. This suggests that the model undergoes a second-order phase transition accompanied by the fluctuation of S_3. If we think that the largest three data of $C_{S_3}^{\max}$ shown in Fig. 7(b) can be fitted to Eq. (8), we have

$$\sigma=0.0879\pm 0.0087. \tag{9}$$

The solid line in Fig. 7(b) is drawn by using the result in Eq. (9). This indicates that the phase transition is very weak, but it is a second-order one.

Hence, it is possible to consider that there is a fixed point of the β function of the model at finite μ, where the correlation length is expected to be divergent, so that all physical quantities become independent of the discrete lattice structure of the model.

However, it is also possible that $C_{S_3}^{\max}$ saturates at $N > 4500$, which are larger than those plotted in Fig. 7(b). Therefore, it is not conclusive that the phase transition is of second order.

Nevertheless, the existence of the peak in C_{S_3} suggests that the model undergoes a phase transition separating the branched polymer phase and the crumpled phase at $\mu \to 0$. It should be noted that this phase transition separates also internally random and flat configurations, which are characterized by $S_3 \neq 0$ and $S_3 = 0$, respectively.

IV. SUMMARY AND CONCLUSION

We studied the phase transitions in the model of two-dimensional surface that was first constructed by Baillie *et al.* for an interpolation between the model of fluid membranes and the model of crystalline membranes. The Hamiltonian of the model is given by $S = S_1 + \mu S_3$, where S_1 is the Gaussian energy and S_3 is the intrinsic squared scalar curvature energy, and μ is the parameter that interpolates the fluid and the crystalline models of membranes. The dynamical variables of the model are the positions of vertices X and the triangulations $\mathcal{T}$. The results are summarized as follows:

The shape of surfaces becomes tubular (i.e., branched polymer) at the intermediate values of μ. The model undergoes a first-order phase transition separating the branched polymer phase and the crumpled phase at $\mu \to \infty$. Moreover, the model undergoes a second- (or higher-) order phase transition between the branched polymer phase and the crumpled phase at $\mu \to 0$.

If the phase transition between the branched polymer phase and the crumpled phase at $\mu \to 0$ is second order, it is characterized by the divergence of the specific heat C_{S_3} at the critical point $\mu_c (\simeq 2.3)$. X^2 continuously changes at this critical point, whether the order of the phase transition is second or higher. The surfaces are also considered to be internally flat at $\mu > \mu_c$ where the coordination numbers σ_i at almost all vertices become 6, while the surfaces become internally at random at $\mu < \mu_c$ where the σ_i are not always 6.

The first-order phase transition is characterized by the discontinuity of X^2, hence by the Hausdorff dimension H; $H \simeq 2$ in the branched polymer phase just below $\mu_c^{1\text{st}}$, while $H \simeq 15$ in the crumpled phase at $\mu > \mu_c^{1\text{st}}$. This phase transition is also characterized by a gap in S_3 at the critical point $\mu_c^{1\text{st}}$.

It would be interesting to study the model defined by the Hamiltonian $S = S_1 + bS_2 + \mu S_3$, where S_2 is the extrinsic curvature (i.e., the bending energy), because this model contains the smooth phase where the surface becomes smooth.

[1] A.M. Polyakov, Nucl. Phys. B **268**, 406 (1986).
[2] H. Kleinert, Phys. Lett. B **174**, 335 (1986).
[3] J.F. Wheater, J. Phys. A **27**, 3323 (1994).
[4] F. David, in *Two Dimensional Quantum Gravity and Random Surfaces*, edited by D. Nelson, T. Piran, and S. Weinberg (World Scientific, Singapore, 1989), Vol. 8, p. 87.
[5] D. Sornette and N. Ostrowsky, in *Micelles, Membranes, Microemulsions, and Monolayers*, edited by W.M. Gelbart, A. Ben-Shaul, and D. Roux (Springer-Verlag, New York, 1994).
[6] A. Ben-Shaul and W.M. Gelbart, in *Micelles, Membranes, Microemulsions, and Monolayers*, 1, edited by W.M. Gelbart, A. Ben-Shaul, and D. Roux (Springer-Verlag, New York, 1994).
[7] Y. Kantor and D.R. Nelson, Phys. Rev. A **36**, 4020 (1987).
[8] Y. Kantor, in *Statistical Mechanics of Membranes and Surfaces*, edited by D. Nelson, T. Piran, and S. Weinberg (World Scientific, Singapore, 1989), Vol. 5, p. 115.
[9] A. Baumgartner and J.S. Ho, Phys. Rev. A **41**, 5747 (1990).
[10] J.S. Ho and A. Baumgartner, Europhys. Lett. **12**, 295 (1990).
[11] G. Gompper and D.M. Kroll, Phys. Rev. E **51**, 514 (1995).
[12] D.H. Boal, U. Seifert, and A. Zilker, Phys. Rev. Lett. **69**, 3405 (1992).
[13] J.F. Wheater, Nucl. Phys. B **458**, 671 (1996).
[14] M. Bowick, S. Catterall, M. Falcioni, G. Thorleifsson, and K. Anagnostopoulos, J. Phys. I **6**, 1321 (1996); Nucl. Phys. B, Proc. Suppl. **47A**, 838 (1996); **53A**, 746 (1997).
[15] H. Koibuchi and M. Yamada, Int. J. Mod. Phys. C **11**, 1509 (2000).
[16] M. Bowick, P. Coddington, L. Han, G. Harris, and E. Marinari, Nucl. Phys. B, Proc. Suppl. **30A**, 795 (1993); Nucl. Phys. B **394**, 791 (1993).
[17] K. Anagnostopoulos, M. Bowick, P. Gottington, M. Falcioni, L. Han, G. Harris, and E. Marinari, Phys. Lett. B **317**, 102 (1993).
[18] J. Ambjorn, A. Irback, J. Jurkiewicz, and B. Petersson, Nucl. Phys. B **393**, 571 (1993).
[19] S.M. Catterall, Phys. Lett. B **220**, 253 (1989).
[20] H. Koibuchi and M. Yamada, Int. J. Mod. Phys. C **11**(3), 441 (2000).
[21] H. Koibuchi, Phys. Lett. A **300**, 586 (2002).
[22] F. David and E. Guitter, Europhys. Lett. **5**, 709 (1988).
[23] M.E.S. Borelli, H. Kleinert, and A.M.J. Schakel, Phys. Lett. A **267**, 201 (2000).
[24] M.E.S. Borelli and H. Kleinert, Europhys. Lett. **53**, 551 (2001).
[25] H. Kleinert, Eur. Phys. J. B **9**, 651 (1999).
[26] C.F. Baillie and D.A. Johnston, Phys. Rev. D **48**, 5025 (1993); **49**, 4139 (1994).
[27] C.F. Baillie, D. Espriu, and D.A. Johnston, Phys. Lett. B **305**, 109 (1993).
[28] C.F. Baillie, A. Irback, W. Janke, and D.A. Johnston, Phys. Lett. B **325**, 45 (1994).
[29] N. Ferguson and J.F. Wheater, Phys. Lett. B **319**, 104 (1993).
[30] R. Friedberg and H.C. Ren, Nucl. Phys. B **235** [FS11], 310 (1984).